J Mater Sci: Mater Med (2010) 21:295–308
DOI 10.1007/s10856-009-3862-6

In vitro and in vivo evaluation of the effects of demineralized bone matrix or calcium sulfate addition to polycaprolactone–bioglass composites

O. Erdemli · O. Çaptug · H. Bilgili · D. Orhan · A. Tezcaner · D. Keskin

Received: 12 May 2009 / Accepted: 22 August 2009 / Published online: 16 September 2009

Abstract The objective of this study was to improve the efficacy of polycaprolactone/bioglass (PCL/BG) bone substitute using demineralized bone matrix (DBM) or calcium sulfate (CS) as a third component. Composite discs involving either DBM or CS were prepared by compression moulding. Bioactivity of discs was evaluated by energy dispersive X-ray spectroscopy (ESCA) and scanning electron microscopy (SEM) following simulated body fluid incubation. The closest Calcium/Phosphate ratio to that of hydroxyl carbonate apatite crystals was observed for PCL/BG/DBM group (1.53) after 15 day incubation. Addition of fillers increased microhardness and compressive modulus of discs. However, after 4 and 6-week PBS incubations, PCL/BG/DBM discs showed significant decrease in modulus (from 266.23 to 54.04 and 33.45 MPa, respectively) in parallel with its highest water uptakes (36.3 and 34.7%). Discs preserved their integrity with only considerable weight loss (7.5–14.5%) in PCL/BG/DBM group. In vitro cytotoxicity tests showed that all discs were biocompatible. Composites were implanted to defects on rabbit humeri. After 7 weeks, new tissue formation and mineralization at bone-implant interface were observed for all implants. Bone mineral densities at interface were higher than that of implant site and negative controls (defects left empty) but lower than healthy bone level. However, microhardness of implant sites was higher than in vitro results indicating in vivo mineralization of implants. Addition of DBM or CS resulted with higher microhardness values at interface region (ca. 650 μm from implant) compared to PCL/BG and negative control. Histological studies revealed that addition of DBM enhanced bone formation around and into implant while CS provided cartilage tissue formation around the implant. From these results, addition of DBM or CS could be suggested to improve bone healing efficacy of PCL/BG composites.

O. Erdemli · A. Tezcaner · D. Keskin (✉)
Department of Engineering Sciences, Middle East Technical University, 06531 Ankara, Turkey
e-mail: dkeskin@metu.edu.tr

O. Çaptug · H. Bilgili
Faculty of Veterinary Medicine, Department of Surgery, Ankara University, 06110 Ankara, Turkey

D. Orhan
Department of Pediatrics, Pathology Unit, Hacettepe University, Ankara, Turkey

A. Tezcaner · D. Keskin
Graduate Department of Biomedical Engineering, Middle East Technical University, 06531 Ankara, Turkey

1 Introduction

Bone is a dynamic tissue that can self-regenerate and self-model under normal physiological conditions. Under some circumstances that result in large bone defects, such as trauma or tumor removal, bone cannot completely heal the defect site. Hence, bone grafting procedures have been developed to provide mechanical or structural support to the bone, and to improve bone tissue formation. Earliest group of materials to be used in bone replacement are calcium sulfates (CS) [1]. However, CS fail to provide long term three-dimensional framework to support osteoconductivity [2]. They are mostly used as bone void fillers and osteoconductive carriers for antibiotics, bone morphogenetic proteins (BMPs) or other bioactive molecules [3]. Demineralized bone matrix (DBM) has also been used as bone grafts [4].

As bone tissue has a composite nature, single phase materials are not able to provide all the biological and mechanical properties necessary for successive bone grafting. The combination of two or more materials with different properties can meet these demands. The potential of bioactive fillers (i.e. calcium phosphate, bioglasses) with biodegradable polymers (i.e. PLGA, PLLA, PCL) as composites have been under investigation by many research groups [5–7].

Poly (ε-caprolactone) is a biocompatible polymer which has long degradation time owing to its high degree of crystallinity and hydrophobicity [8, 9]. PCL releases non-toxic by-products upon hydrolytic in vivo degradation [9] and does not generate an acid environment unlike the polylactide (PLA) or polyglycolide (PLG) polymers due to its slow degradation [10]. PCL had been approved by the Food and Drug Administration for human clinical use in vivo [11, 12]. However, for bone repair applications, reinforcement of PCL is necessary to improve its mechanical properties [13]. For this purpose, PCL has been either blended with other polymers, such as PLA and PLGA, [12, 14] or reinforced with bioceramics, like HA, bioglasses [15–17]. The purpose of the use of bioactive fillers (i.e. tricalcium phosphates, calcium carbonates) with PCL also involves augmenting bone healing through enhanced osteoconduction [18].

Bioglasses are silica glasses with a specific composition of SiO_2, Na_2O, CaO and P_2O_5. Their biocompatibility, osteoconductivity, and osteoinductivity have been well documented [6, 19]. Bioglasses have the ability to form bone-like apatite structures and develop mechanically stable organic bonds to the bone in the presence of biological fluids. These bioactive glasses are used in maxillofacial reconstruction, dental applications, in coating of orthopedic prostheses and as fillers for bone defects [20–22].

The purpose of this study is to improve the efficacy of polycaprolactone/bioglass (PCL/BG) bone substitute using demineralized bone matrix or calcium sulfate as a third component. In PCL/BG, PCL/BG/CS and PCL/BG/DBM discs, the slow degradation of PCL was expected to maintain an adequate union and mild inflammatory reactions at the bone implant interface considering the long healing process of bone.

2 Materials and methods

2.1 Preparation of PCL-bioglass based composite discs

Bioglass (Perioglass®, US Biomaterials, USA), calcium sulfate (Sigma–Aldrich, Germany), and demineralized bone matrix® (DBM, LifeNet, USA)—were ground using a Ceramic Ball Mill (Retsch MM200, Germany) before disc preparation. Poly(ε-caprolactone) (M_w = 14,000 Da, Sigma–Aldrich, Germany) was first heated on a Teflon sheet to about 55°C. BG, a well-known osteoconductive material, was then added to the polymer as the bioactive filler for enhancement of mechanical strength of PCL as well as for decreasing the polymer partition in discs. After cooling down to about 40°C the third component (DBM or CS) was mixed thoroughly. The mixture was transferred to a metal mould and compressed under 2000 N load for 5 min. Compression moulding after mixing molten PCL with fillers was chosen as the processing technique to eliminate the solvents and minimize the inflammatory responses besides ensuring homogenous mixing of all components. PCL/BG, PCL/BG/CS and PCL/BG/DBM discs (ca. 5 × 2 mm in diameter and height, respectively, Fig. 1) were prepared with compositions: PCL/BG (2.5:1, w/w), PCL/BG/CS (2.5:1:1, w/w), and PCL/BG/DBM (2.5:1:1, w/w). The discs were stored at 4°C in a desiccator until use.

2.2 Bioactivity analysis

Surface mineralization of the discs was evaluated by incubating in simulated body fluid (SBF) for 1, 7 and 15 days at 37°C. SBF was prepared according to the work of Müller et al. [23]. The bioactivity of only PCL containing discs was also studied for different time periods. At the end of incubations, discs were coated with a gold–palladium alloy for analysis with scanning electron microscopy (SEM; JSM-6400 Electron Microscope, Japan). The Ca/P ratio and the elemental composition of the apatite layer formed on disc surfaces were determined by X-ray Photoelectron Spectroscopy (XPS). XPS analysis was carried out on an ESCA System with Mg/Al dual anode (SPECS, Germany) by using a Mg Kα radiation.

2.3 In vitro degradation of discs

For degradation studies six discs from each group were incubated in phosphate buffered saline (PBS) solution (10 mM, pH 7.4) at 37°C in a shaking water bath for 4 and 6 weeks. To evaluate and compare the degradation behavior of discs; structural integrity, water uptake, weight

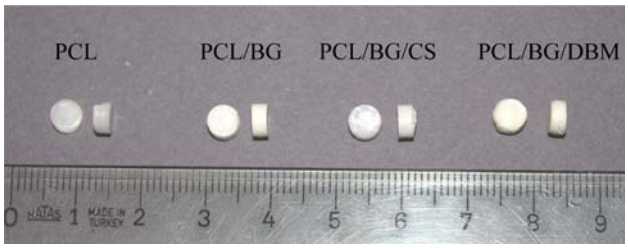

Fig. 1 Photographs of the discs

loss, and mechanical properties were studied after each incubation period.

Weight loss was calculated as the percent change in dry weight as shown in Eq. 1:

$$\text{Weight loss}(\%) = \frac{W_i - W_t}{W_i} \times 100 \quad (1)$$

where, W_i is the initial and W_t is the final dry weights.

The water uptake for each incubation period was calculated according to the Eq. 2:

$$\text{Water uptake}(\%) = \frac{W_w - W_i}{W_i} \times 100 \quad (2)$$

where, W_i is the initial dry weight and W_w is the wet weight at the end of incubation period.

2.4 Mechanical testing

The mechanical properties of six discs of each group upon incubations in PBS were evaluated by both microhardness and compression tests. The microhardness values of discs were measured by a microhardness tester (Wilson Tukon Series A240 RHT, England). Vickers indenter was used and a load of 0.05 kgf was applied with a 5 s dwell time in the tangential direction to the examined area [24]. The indentation was applied to 12 points on the surfaces of PCL/BG, PCL/BG/CS and PCL/BG/DBM and PCL discs. The Universal testing machine (LR50 K Lloyd Instruments, UK) with Nexygen MT Software (Ametek Inc., UK) was used for the compression tests (crosshead speed of 1 mm/min, 2.5 kN load cell). Six discs from each group were used as zero time controls. The compressive modulus (Young's modulus) was calculated from the initial elastic region of the stress–strain curves obtained from the compression tests.

2.5 In vitro cytotoxicity studies

Biocompatibility of discs was evaluated using in vitro cytotoxicity tests in accordance with ISO 10993-5: 1999. The human osteosarcoma cell line (Saos-2) was routinely cultured in Dulbecco's modified Eagle's medium (DMEM), supplemented with 10% (v/v) fetal bovine serum, 1% (v/v) sodium pyruvate solution and 10 U/ml penicillin/streptomycin. All cell culture reagents were the products of PAA (Austria). For the proliferation studies, 50,000 cells/disc were seeded on each disc and cultured in osteogenic medium [25]. Discs without cells were used as blank and cell seeded tissue culture wells served as controls. After 4 and 10 days of incubation, MTT (3-{4,5-dimethylthiazol-2yl}-2,5-diphenyl-2H-tetrazolium-bromide) assay was done to study the proliferation of the cells on the discs. Shortly, discs were incubated with MTT (Gerbu Biotechnik, Germany) for 4 h at 37°C in a carbon dioxide incubator (5215 Shel Lab., USA). MTT was taken up by viable cells and reduced to insoluble purple formazan crystal by their dehydrogenase enzymes. At the end of the incubation, MTT solution was removed, discs were rinsed with PBS. DMSO solution was added onto discs to solubilize formazan crystals formed inside the cells. The absorbance was measured at 550 nm with microplate spectrophotometer (μQuant, Biotek Ins. Inc., USA). The cells were also fixed with 4% glutaraldehyde, and air-dried for SEM analysis.

2.6 In vivo applications of PCL-bioglass based discs

2.6.1 Animals and surgery

For in vivo applications, 13 white male rabbits (2–2.5 kg) were used. The experimental groups used for in vivo studies are given in Fig. 2. The procedures on animals were performed in accordance with ethical guide lines for Animal Care and Ethics Committee of the Ankara University, Faculty of Veterinary Medicine. Rabbits were anesthetized using an intramuscular injection of the combination of 2 mg/kg body weight xylazine hydrochloride (Egevet, Turkey) and 10 mg/kg body weight ketamine hydrochloride (Egevet, Turkey) before surgery. Single unicortical bone defect (5 mm in diameter) was created at the 1/3 diaphyseal proximal region of both humeri of all experimental groups by using a motorized drill and the implants were anchored by press-fitting them into these holes. The bone defects were either filled with discs ($n = 5$ for each group) or left empty (negative control, $n = 5$) (Fig. 2). As positive control, rabbits had anesthesia and incision of the skin-muscle tissues at 1/3 diaphyseal proximal region of both humeri. They were then sutured without creating any bone defect. After surgery, the rabbits were kept caged freely in standard rabbit cages and given their usual regime of food and water. Neo-terramycin (Pfizer, Turkey) was given postoperatively to the rabbits. The rabbits were sacrificed after 50 days using overdosage of thipentotal-Pentotal (Abbott, Italy). The humeri were then removed, placed in separate tubes as wrapped in saline soaked gauze sponge. Samples were stored at −20°C until QCT, SEM, radiology and biomechanical analysis.

2.6.2 Radiological evaluation

Conventional X-rays were obtained on Kodak Medical X-Ray general purpose film (USA) with Innomed X-ray machine (Top-X HF Model 2003, USA). The distance of the X-ray source to the bones was 75 cm. The setting of the machine was 40 kV, 50 mA and 0.5 s. Defect healing in terms of bone formation was graded from 0 to 4. In case of no bone formation at the defect site, it was graded as zero.

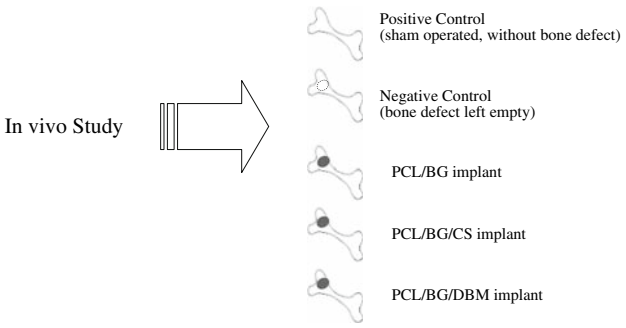

Fig. 2 Experimental groups for in vivo studies

Bone formation in terms of 1/4, 2/4, 3/4 and 4/4 coverage of the defect were graded as 1, 2, 3, and 4, respectively. Two orthopedists with no prior knowledge about the groups graded the X-rays.

2.6.3 Quantitative computed tomography (QCT)

The bone mineral densities (BMD) were analyzed by quantitative computed tomography (QCT) using a Phillips Tomoscan 60/TX third generation scanner (Phillips, USA). The density values were calculated from the calibration curve constructed with the average of attenuation numbers (CT numbers) of different materials with known densities. The CT number is a normalized value of the calculated X-ray absorption coefficient of a pixel in a computed tomogram.

2.6.4 Microhardness tests

The humeri were moulded into an acrylic polymer using AcryFix kit (Struers, Denmark). They were then cut into small discs (ca. 10×4 mm in diameter and height, respectively) through the implant region using a low speed diamond saw (Isomet, Buehler, USA). The microhardness values were measured by a microhardness tester with the same procedure used for the PCL/BG, PCL/BG/CS and PCL/BG/DBM discs. The indentation was applied to 6 points on the positive (humeri of positive control) and 6 points on the negative control (empty defect) groups. 18 points (6 at intact bone, 4 at implant region, and 8 at bone/implant interfaces) were used for implant groups. The measurements at interface were described for the two regions; interface I (ca. 150 μm from the implant) and interface II (ca. 650 μm from the implant).

2.6.5 Scanning electron microscopy (SEM)

After being coated with gold, cross-sections of humeri ($n = 3$) at the implant sites were analyzed by SEM for the apatite formation at bone-implant interfaces and osteointegration of implants.

2.6.6 Histological examination

Freshly harvested bones were fixed in 4% formalin for 1 day at room temperature, decalcified in 30% formic acid for 48 h (Sigma–Aldrich, Germany) and embedded in paraffin at 30°C for 15 min after dehydration through a series of graded ethanol (70–100%). The 4 μm sectioned samples were stained with hematoxylin and eosin for morphological examination (Zeiss LSM510, Confocal Microscope). The samples were then examined and photographed for histological evaluation as described in the previous study of Shao et al. [26].

2.7 Statistical analysis

In comparing the groups for a single parameter one-way ANOVA test was used with Tukey's Multiple Comparison Test for the post-hoc pairwise comparisons (SPSS-9 Software Programme, SPSS Inc., USA). Differences were considered significant for $P < 0.05$.

3 Results

3.1 In vitro characterization of discs

3.1.1 Analysis of apatite formation on disc surfaces

After SBF incubations, PCL/BG, PCL/BG/CS and PCL/BG/DBM discs were covered by crystal structures at several regions of the surface after 1 week (Fig. 3a–f). However, there was no apatite formation on the surface of only PCL containing discs (Fig. 3g). Ca–P precipitates formed on the surfaces of PCL/BG, PCL/BG/CS and PCL/BG/DBM discs were granular in shape and similar in size.

XPS analysis was used to determine the composition of the formations on the surface of the discs. The binding energies determined for C 1s, O 1s, P 2p and Ca 2p were obtained at Mg anode (1253.6 eV) [27, 28]. Representative XPS survey spectra of PCL/BG/DBM before and after 15 day SBF incubation are given in Fig. 4. The relative compositons of all disc surfaces and Ca/P ratios calculated from XPS spectra are given in Table 1. No Ca 2p and P 2p peaks were present in XPS spectra of PCL alone discs. A significant decrease in C 1s peaks and its atomic percentage was observed while an increase in Ca 2p and P 2p peaks and their percentages were observed with incubation in SBF for PCL/BG, PCL/BG/CS and PCL/BG/DBM groups. Quantitative elemental analysis showed that Ca/P atomic

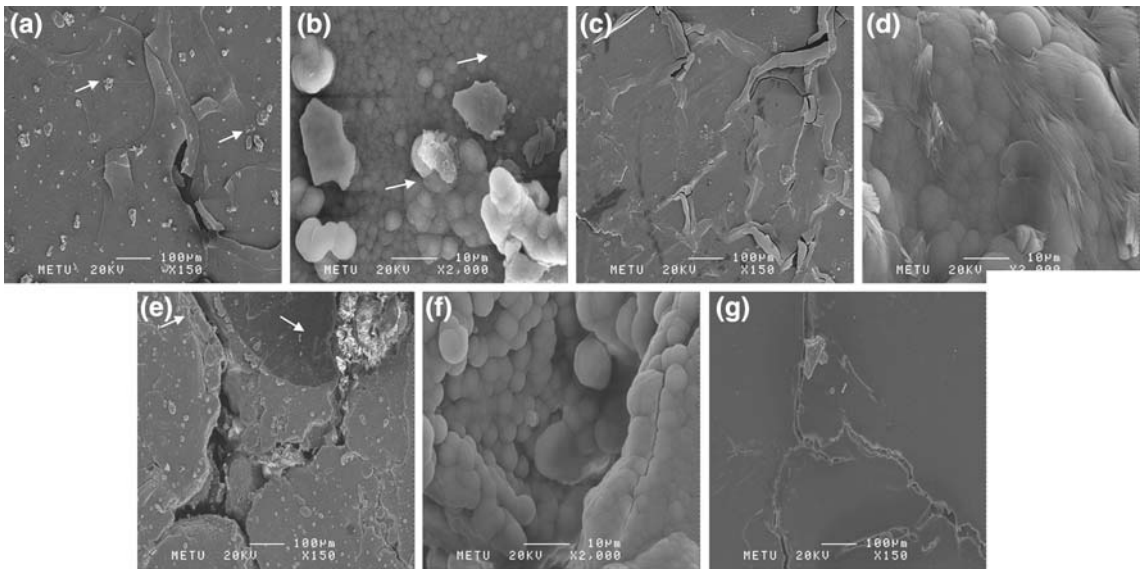

Fig. 3 SEM micrographs of apatite-like crystals formed on the surface of **a** and **b** PCL/BG, **c** and **d** PCL/BG/CS, **e** and **f** PCL/BG/DBM composite discs at different magnifications, **g** PCL alone, after 7 days of incubation in SBF at 37°C. Arrows indicate the apatite-like crystals

ratio was highest for PCL/BG/DBM (1.53) followed by PCL/BG/CS group (1.42).

3.1.2 In vitro degradation analysis

The water uptake and weight loss results of discs are shown in Fig. 5. With the addition of fillers (BG, CS or DBM) increase in water uptake was observed. The PCL/BG/DBM group had significantly higher water uptake percentages (36.25 ± 3.39 and 34.71 ± 4.80%) compared to other groups (PCL: 3.11 ± 0.81% and 4.16 ± 0.85%; PCL/BG: 6.27 ± 1.19% and 6.54 ± 1.51%, and PCL/BG/CS: 7.50 ± 1.74% and 7.19 ± 1.51% after 4 and 6 weeks, respectively). The highest weight loss was observed in PCL/BG/DBM group (7.58 ± 0.80% and 14.47 ± 1.16% for 4 and 6 weeks, respectively). However, PCL discs had almost no change in weight after 4 and 6 week incubations (0.80 ± 0.59% and 1.10 ± 0.36%, respectively).

3.1.3 Evaluation of the mechanical properties of PCL based discs

It was observed that the addition of organic (DBM) and inorganic (CS and/or BG) fillers increased the microhardness of PCL discs at zero time (Fig. 6). Microhardness of PCL (8.61 ± 1.22 MPa) and PCL/BG/DBM (8.59 ± 0.98 MPa) were significantly lower than the other two groups after 4 weeks. However, at the end of 6 week incubations PCL/BG/DBM group had the highest microhardness value (7.89 ± 0.87 MPa).

The comparison of the Young moduli of groups for different incubation periods is presented in Fig. 7. At zero time, PCL/BG/DBM group showed the highest compressive modulus (266.23 ± 7.82 MPa) which was followed by PCL/BG/CS (253.92 ± 13.43 MPa). PCL/BG and PCL alone groups showed smaller moduli values at both incubations than that of PCL/BG/CS. While the compressive moduli of PCL/BG/DBM discs decreased from 266.23 ± 7.82 to 54.04 ± 6.47 MPa at the end of 4 weeks, no significant change was observed for the other groups. However, PCL/BG/CS discs' moduli also decreased from 253.92 ± 13.43 to 183.89 ± 4.55 MPa after 6-week incubations. PCL/BG group showed almost no change in compressive modulus after the incubations.

3.1.4 In vitro cytotoxicity studies

Saos-2 cells continued to proliferate on all discs except PCL discs after 4 days (Fig. 8). MTT results for PCL/BG and PCL/BG/DBM groups were found statistically indifferent than positive control group ($P \geq 0.05$). The SEM examinations showed that cells attached onto PCL/BG and PCL/BG/DBM discs were spread (Fig. 9a, b) while on PCL/BG/CS and PCL discs (Fig. 9c, d) they were round in morphology. However, among the round cells on PCL/BG/CS discs, crystal structures were also observed. SEM examination revealed that the degree of proliferation on PCL discs was lower than all other groups.

3.2 In vivo studies

After removal of humeri, the general appearances of the implant (operation) regions were examined macroscopically. The defect regions were found either totally or

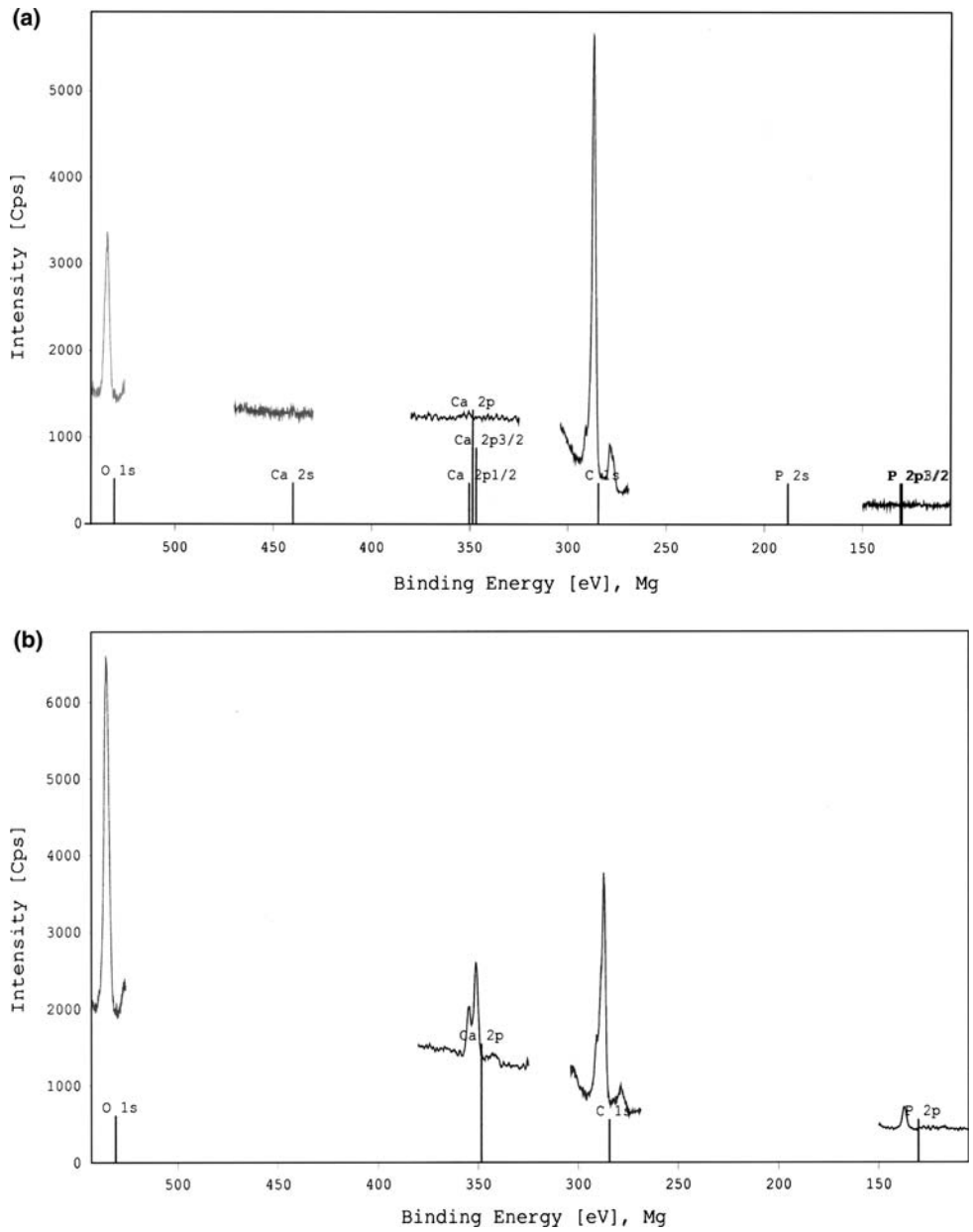

Fig. 4 XPS analysis of PCL/BG/DBM **a** before, **b** after 15-day incubation in SBF at 37°C

partially occupied by discs. Formed tissue at the empty-defect site was different in appearance (darker in color, non-uniform), compared to the healthy bone. In all implant groups the operation area was covered with fibrous tissue with varying thicknesses.

3.2.1 Radiological evaluations

Radiographs showed that the defect sites were visible for the negative control but almost undistinguishable in most of the PCL/BG, PCL/BG/CS and PCL/BG/DBM groups (data not shown). Radiological scoring for bone formation at the implant sites were higher than that of negative control but lower than positive control (Table 3). It was also observed that negative control had significantly lower bone formation at the defect site than the cortex of positive control.

3.2.2 Comparison of bone densities by quantitative computed tomography (QCT)

The comparative results of bone densities for implant regions and bone-implant interfaces are given in Table 2. All implant groups had significantly higher BMD values

Table 1 Quantitative surface chemical composition of composites discs before and after 7 and 15 days SBF incubations at 37°C and Ca/P ratios calculated from XPS analysis

Element	at.% PCL zero time	at.% PCL/BG zero time	at.% PCL/BG/CS zero time	at.% PCL/BG/DBM zero time
C	78.90	79.20	81.10	85.80
O	21.00	19.90	18.60	13.60
P	0.00	0.70	0.10	0.20
Ca	0.00	0.20	0.10	0.40
Ca/P ratio	0.00	0.29	1.00	2.00
	PCL day 7	PCL/BG day 7	PCL/BG/CS day 7	PCL/BG/DBM day 7
C	77.30	48.00	46.00	66.10
O	21.9	36.90	39.20	29.30
P	0.40	6.80	6.30	1.70
Ca	0.40	8.30	8.60	3.00
Ca/P ratio	1.00	1.22	1.37	1.77
	PCL day 15	PCL/BG day 15	PCL/BG/CS day 15	PCL/BG/DBM day 15
C	70.50	56.70	47.50	59.40
O	25.10	32.10	38.10	32.50
P	1.90	4.90	5.90	3.20
Ca	2.50	6.30	8.40	4.90
Ca/P ratio	1.32	1.29	1.42	1.53

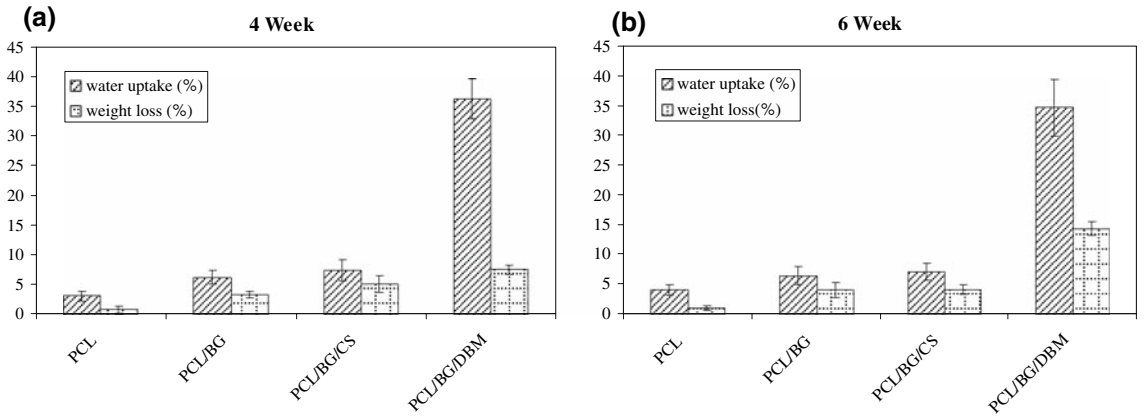

Fig. 5 The water uptake and weight loss of the composite discs after in vitro incubations for **a** 4 and **b** 6-week incubation periods

than the defect region of the negative control. However, there were also statistically significant differences between positive control and all other groups. Only in PCL/BG group BMD value of the interface region was significantly higher than the implant region.

3.2.3 Microhardness test results

When the hardness values of implant, bone and interface regions were examined, it was found that there was an increase in the microhardness values towards the healthy bone tissue in accordance with the distance from the implant (Fig. 10a, b). Figure 10a shows that PCL/BG had significantly lower microhardness than both PCL/BG/DBM and negative control groups in implant regions ($P < 0.05$ level). The microhardness values of bone-implant interface II of all implant groups were found significantly higher than that of negative and lower than that of positive controls. The microhardness values of interface II were found significantly higher than those of interface I for all implant groups, except PCL/BG (Fig. 10a, b). The highest increase in microhardness was observed for PCL/BG/CS (3.94 fold), followed by PCL/BG/DBM (2.62 fold).

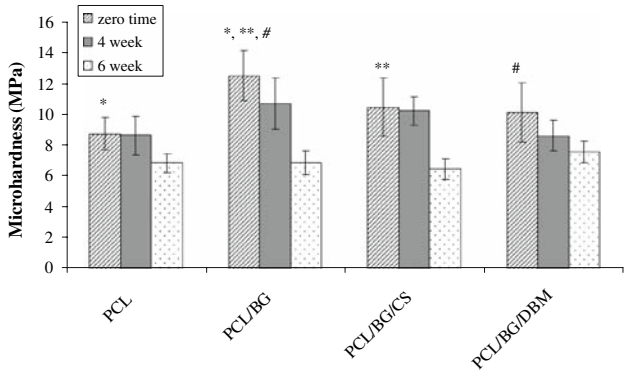

Fig. 6 The comparison of the microhardness values of disc surfaces after in vitro incubations. (Statistical significant differences were labeled in the figure only for zero time results. Statistical significances were at $P < 0.05$ level, $n = 6$)

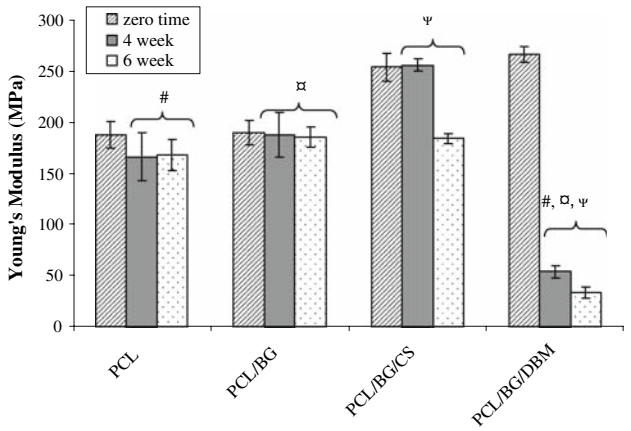

Fig. 7 Young's moduli of discs incubated in PBS for different time periods. (Statistical significant differences were labeled in the figure only for the 4 and 6 week results of PCL/BG/DBM discs; being different from all groups. Although not shown in the figure at zero time both PCL and PCL/BG were statistically significantly lower than the PCL/BG/CS and PCL/BG/DBM groups. At 4 weeks PCL/BG/CS discs had the statistically highest compressive modulus values. However, this value decreased to the level of PCL and PCL/BG group at 6th week. Statistical significances were at $P < 0.05$ level, $n = 6$)

3.2.4 SEM analysis

SEM examinations showed that positive control group had healthy compact bone with dense and smooth appearance (Fig. 11a). A highly porous bone-like structure has been observed in negative control at the defect site (Fig. 11b). Apatite-like crystals similar to SBF results (Fig. 3) were observed more at the implant bone interface of PCL/BG group (Fig. 11c). A distinct separation of PCL/BG/CS implant from the bone was observed during SEM analysis (Fig. 11d). PCL/BG/DBM group showed a physically indistinguishable interface with bone tissue as given in Fig. 11e.

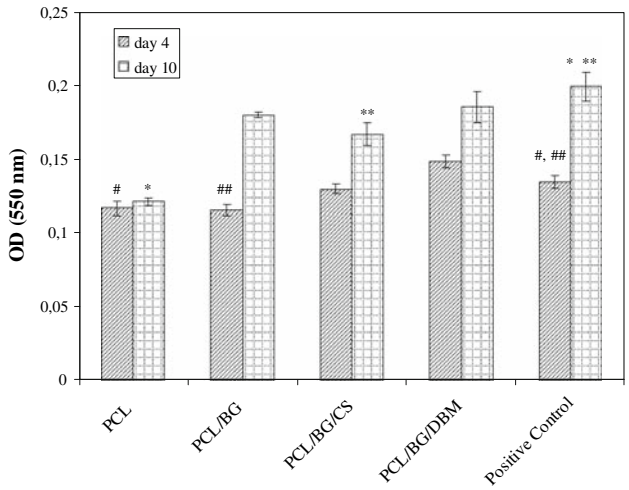

Fig. 8 The proliferation of Saos-2 cells on the disc surfaces. Only statistical significant differences from the positive control were shown in the figure. Only PCL group was different from positive control for both time periods, PCL/BG group was found statistically different from positive control for 4 day results and PCL/BG/CS group was different from positive control for 10 day results. PCL group was different from all composite groups for all both time results except PCL/BG group's 4 day result. Statistical significances were at $P < 0.05$ level

3.2.5 Histological findings

Histological analysis of humeri sections showed that there were no inflammatory signs and adverse tissue reaction in all groups (Fig. 12). PCL/BG implants showed osteoblastic activity at the bone-implant interface as a result of osteoconductive property of BG (Fig. 12a, e, i). At the PCL/BG/CS bone-implant interface, new cartilage formation was examined but the cellular arrangement in new tissue was unorganized (Fig. 12b). This group also showed osteoblastic activity towards the inside of implants which was more clear at higher magnifications (Fig. 12f, j) Implant was surrounded by host bone with close apposition which showed the integration of bone and PCL/BG/DBM disc (Fig. 12g, k). When the negative control group was examined, unorganized porous tissue formation was observed at defect site around the remnants of bone (Fig. 12d). The porosity of the new tissue was more clear at higher magnifications (Fig. 12h, l).

4 Discussion

The ability of bonding of an implant with the bone, important for its success, is done through the apatite layer formation on their surfaces [29]. The apatite precursor (HCA) structures observed by SEM on the surface of PCL/BG, PCL/BG/CS and PCL/BG/DBM discs (Fig. 3a–f) were similar in appearance to those in related studies [30, 31].

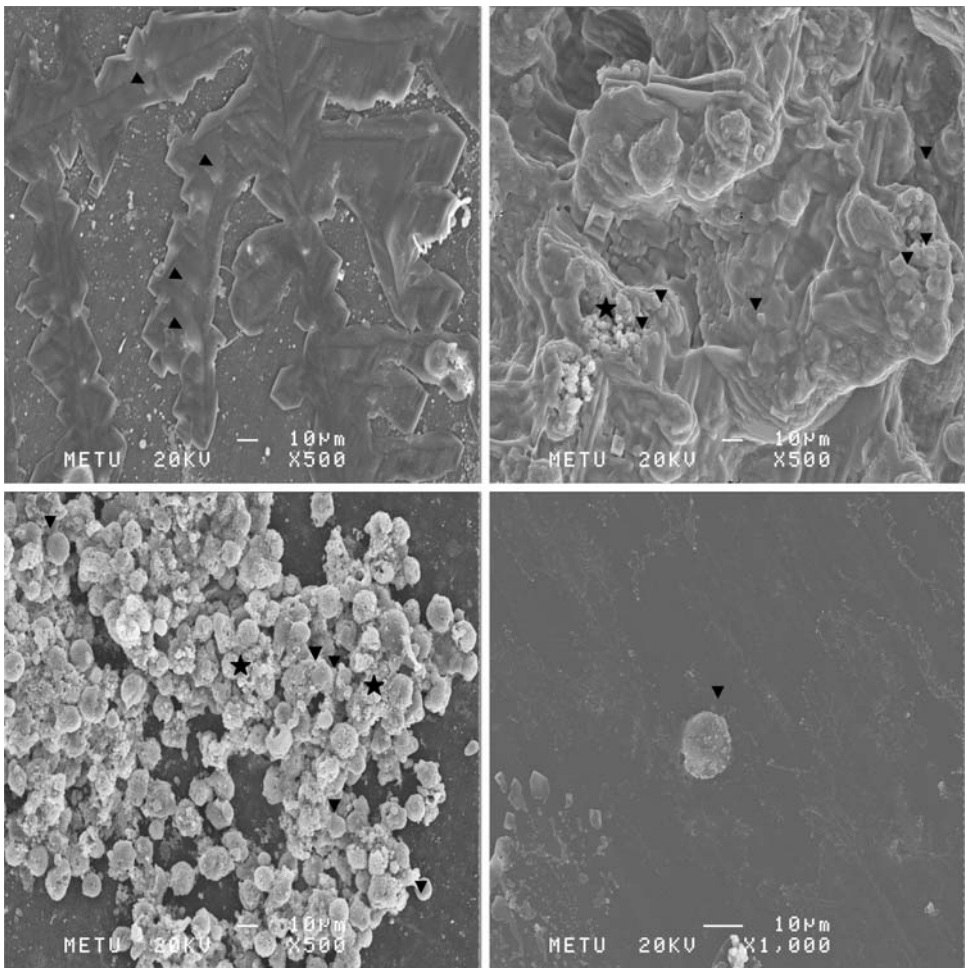

Fig. 9 SEM micrographs of Saos-2 cells seeded on the surface of **a** PCL/BG, **b** PCL/BG/DBM, **c** PCL/BG/CS composite discs, **d** PCL alone after 10 days of incubation in osteogenic medium. Arrow heads show single or a group of cells. Stars are used to show apaptite like depositions

Table 2 Bone mineral density (BMD) of implant regions and bone-implant interfaces ($n = 4$)

Groups	Bone mineral density (g/cm^3)	
	Implant region	Bone-implant Interface
PCL/BG	1.618 ± 0.053*	1.709 ± 0.046*
PCL/BG/DBM	1.585 ± 0.082	1.637 ± 0.074
PCL/BG/CS	1.635 ± 0.080	1.677 ± 0.094
Negative control	1.281 ± 0.013	
Positive control	2.028 ± 0.062	

* Indicates the significant difference between interfaces and implant regions of PCL/BG group ($P < 0.05$)

As no such structures were observed on only PCL containing discs (Fig. 4g), it can be suggested that HCA formation occurred as a result of the presence of fillers (BG, CS, and DBM). SEM and XPS analyses also showed deposition of Ca and P containing crystals on the surfaces. Quantitative surface analysis revealed that PCL/BG/DBM discs (at 15 day) had a Ca/P atomic ratio closest to that of HCA shown by Gu et al. [27]. Thus, addition of third component resulted with an increase in the deposition of apatite-like crystals improving the bioactivity of the discs.

The highest water uptake observed for DBM containing group was expected from its high collagen content that has high swelling properties [32]. However, this property was also the cause of microcrack formation, resulting in significant weight losses only in this group. The effect of these microcracks was also observed in compression test results with a sharp decrease in modulus of DBM containing group. Similar decline modulus was observed later (in 6 weeks) for PCL/BG/CS group, despite its lower swelling and weight loss values. This was because of hydrophilic nature of CS that enabled water diffusion into the discs. In contrary to this low hydrophilicity of BG caused less water permeation into the discs resulting in small decrease in modulus in time. However, PCL/BG discs, also had lower initial modulus than the PCL/BG/CS and PCL/BG/DBM groups owing to poor filler properties of bioglass. Hence the third components enhanced the mechanical properties with PCL/BG/CS having highest modulus after 4 weeks implantation. Enhancement of surface microhardness was observed with the addition of all

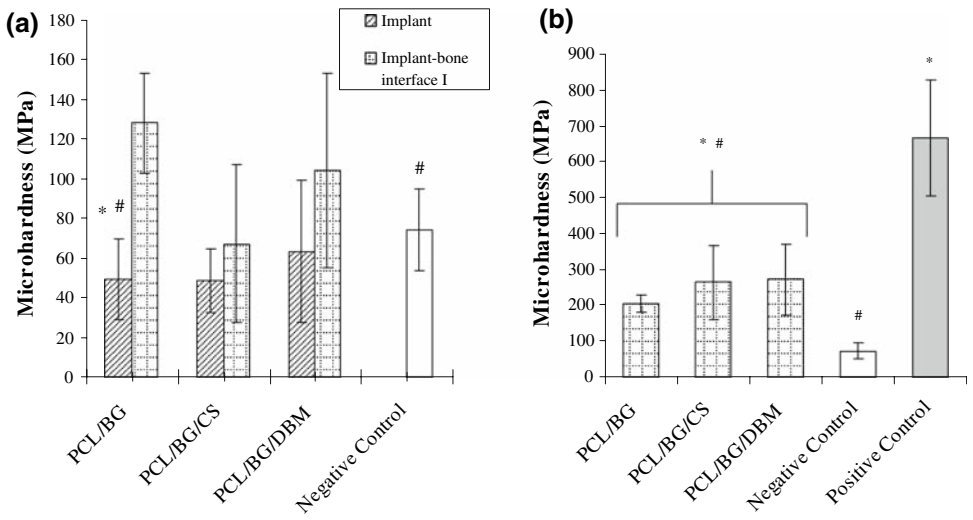

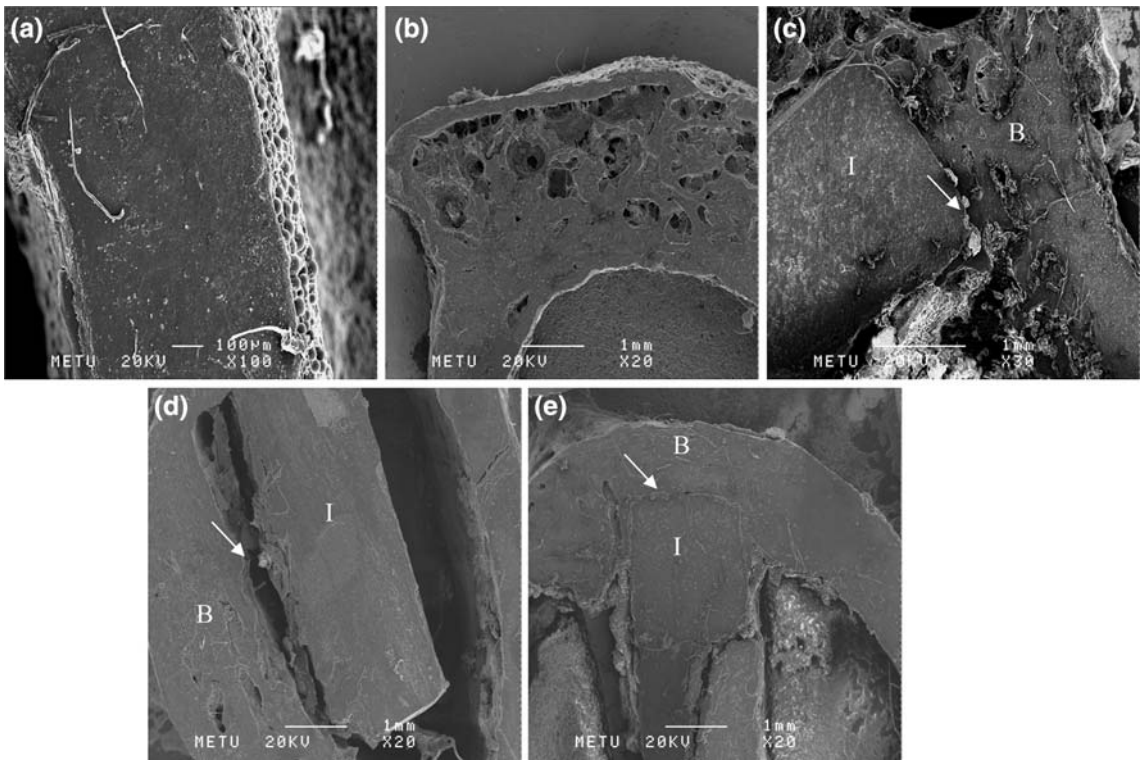

Fig. 10 The comparison of the microhardness values of **a** implant and bone-implant interface I, **b** bone-interface II and empty defect (negative control) and healthy bone after in vivo application. Negative control was the microhardness at the defect site after 7 weeks of healing when left empty

Fig. 11 General SEM micrographs of the crosssections of bone implant interfaces after in vivo applications **a** Positive control-no defect created on bone, **b** Negative control-empty defect, **c** PCL/BG disc applied to bone defect, **d** PCL/BG/CS disc applied bone defect, **e** PCL/BG/DBM disc applied bone defect, (I, implant; B, bone; arrow, bone implant interfaces). Separation at bone-implant interface for CS containing group was thought to be related with specimen preparation process

fillers. It was more pronounced in PCL/BG group that has highest BG component (Fig. 6). Decrease in microhardness values upon incubations could be explained by loss of these components (BG, CS, DBM) from the surface either by dissolution or via physical detachment.

The small weight changes observed in all groups was related with slow degradation of PCL that involves random hydrolytic scission of the ester groups in amorphous regions with water diffusion in its early stage [7]. It has been shown in literature that implants of high molecular weight PCL (66,000 Da) placed subcutaneously had degraded to 15,000 Da in 24 months but after that, molecular weight decreased to 8,000 Da within 6 months. The implants had been found as small pieces which can not be distinguished after 6 additional months [33]. Accordingly, as the molecular weight of PCL used in the current

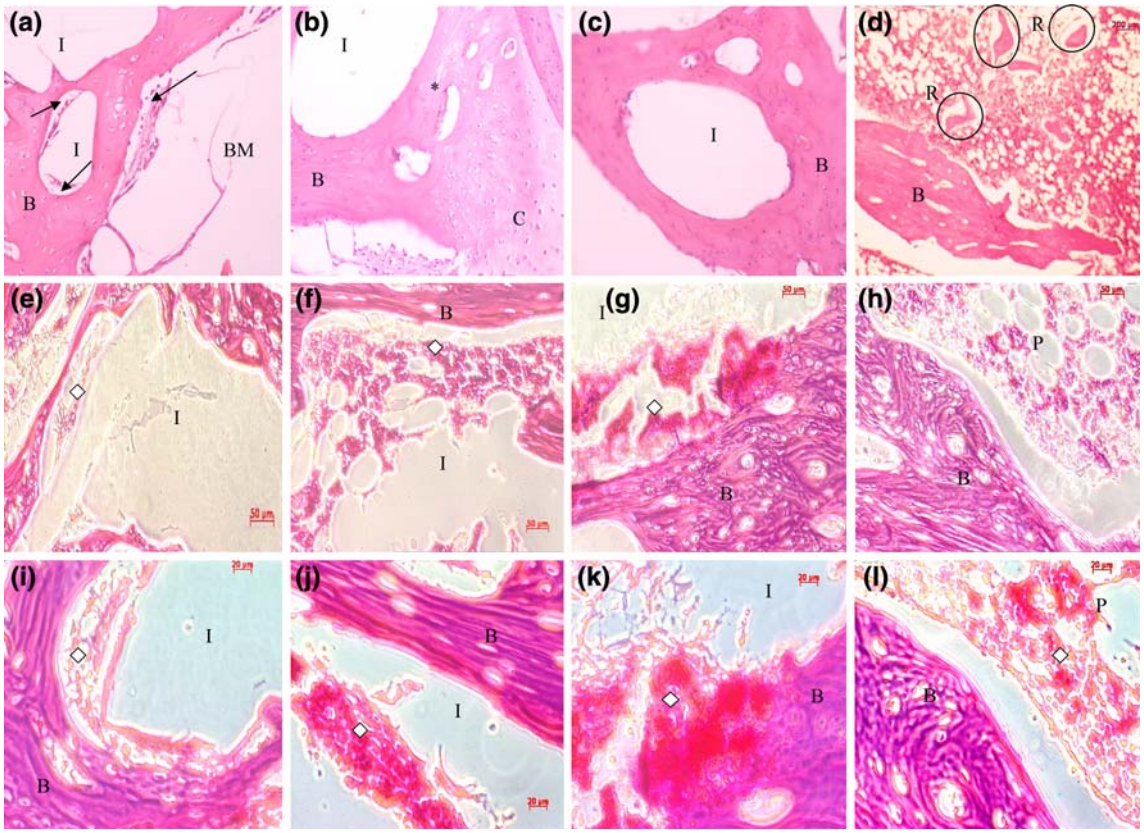

Fig. 12 Light micrographs of the histological sections of bone implant interface after in vivo applications **a** PCL/BG, **b** PCL/BG/CS, **c** PCL/BG/DBM and **d** Negative control-empty defect (HE, original magnification: 4×). I: Implant Region; B: Host Bone; BM: Bone Marrow; C: Cartilage Region, R and P: Remnants of bone and porous new tissue formation at the defect site in the negative control; Arrow: Osteoblastic Activity; * Unorganized Cartilage, Diamond: new tissue formation. **e–h** 20× magnification, **i–l** 40× magnification of groups with respect to the order of top row

study is small (14,000 Da), and it is used together with other components (at almost equal ratio, 2.5:1:1), it is expected to degrade faster than pure or high molecular weight PCL implants. As bone healing is a longer time requiring process, these PCL based composites are considered advantageous for giving mechanical support during healing period.

In vitro cytotoxicity tests demonstrated that the activity of cells increased with time except for only PCL group (Fig. 8). The addition of BG, CS and DBM increased the proliferation of the cells on these discs compared to pure PCL. Similarly, to improve the cell attachment and proliferation, PCL is blended with natural components like hydroxyapatite to constitute a natural substrate for osteoblast growth [5, 34]. Highest cell proliferation was observed on DBM containing group which is considered to be due to both osteoconductive and osteoinductive properties of DBM. SEM examinations were in agreement with MTT proliferation results. The cell morphology observed on PCL/BG and PCL/BG/DBM discs suggest that the surface properties of these composites were more suitable for spreading.

For the in vivo applications, considering significant decrease in mechanical properties of PCL/BG, PCL/BG/CS and PCL/BG/DBM composites, humeri was chosen for implantation as it is a less load bearing site than femur. Similarly, Clark et al. chose rabbit proximal humerus instead of tibia or femur models because of low incidence of bone fracture of the humerus [35]. Thus, it is thought that considering humerus anatomy, 5 mm partial cortical bone defect model was suitable for in vivo applications to evaluate usability of these material at less or no load bearing sites.

According to QCT and X-ray analyses of extracted humeri (Tables 2 and 3), new bone formation at bone-implant interface and within the implant has started in all implant groups, but their BMD values and radiological scorings were lower than the positive controls. Among PCL/BG, PCL/BG/CS and PCL/BG/DBM groups there was no significant difference in these values. Only for PCL/BG group, there was a significant BMD increase from implant region to interface region. This high density result for only BG involving group might indicate the higher amount of HCA formation around these implants as

Table 3 Radiological scoring of harvested bones ($n = 4$)

Groups	Bone formation
PCL/BG	3.0 ± 0.82
PCL/BG/DBM	3.0 ± 0.00
PCL/BG/CS	2.8 ± 0.50
Negative Control	2.3 ± 0.96*
Positive Control	4.0 ± 0.00*

* Significant differences between groups ($P < 0.05$)

observed in SEM images (Fig. 10c) and microhardness difference between interface I and implant (Fig. 10a). For negative control group, the BMD value was low indicating the low density-highly porous-bone formation at the defect site in agreement with SEM and histological examinations (Figs. 11, 12). Formation of a woven bone structure (callus) was an expected result of incomplete removal of bone debris as stated by other researchers [36].

Microhardness testing is widely used to evaluate the degree and quality of bone mineralization at bone-implant interface and implant regions after in vivo applications. Microhardness values of all implant regions were higher (i.e. 49 ± 16.2 for PCL/BG/CS) than the implants' zero time and 6 week incubation values (i.e. 10.45 ± 1.87 and 6.30 ± 0.81 for PCL/BG/CS, respectively) observed with in vitro studies (Figs 6, 10a). This shows that although not easily recognizable by SEM, there must have been a considerable mineralization inside the implant after 7 weeks. PCL/BG/DBM implants had the highest microhardness value among implant groups indicating higher new bone formation within the implant due to the presence of bone inductive components of DBM. Although the highest microhardness was observed in interface I region of PCL/BG composites, in interface II region, the DBM and CS containing groups had higher microhardness values. Thus, the positive contribution of third components was observed in agreement with the in vitro results. The distance related increases in microhardness values indicated that bone healing has begun at the bone site, but not reached to the healthy bone level in terms of bone strength. Similar results in terms of bone strength and closeness to the healthy bone were also documented by several research groups [24, 37]. Fini et al. [24] showed that there were significant differences between microhardness data measured at different distance from bone to PMMA/α-TCP implants placed in cortical bone of rabbit models [24]. Aldini and co-researchers [37] studied the osseointegration of the zirconia coated or uncoated bioglass after implantation to the distal femoral epiphyses and found higher microhardness values for the regions closer to the bone at the interface [37].

According to SEM and histological examinations, there was no fibrosis and no giant cells around the implants. This shows that there was neither foreign body reaction nor inflammation around the implants. Similarly, in literature, minor or no foreign body reaction was observed at PCL based implants at 4–16 weeks post-implantation due to their slow degradation [38–40]. Lam et al. [41] has studied PCL and PCL-based scaffolds in a rabbit model (intramuscular and subcutaneous) for up to 6 months and also carried out a preliminary long-term study (2 years) on reconstruction of a critical-sized defect in rabbit calvaria with these scaffolds. They showed good biocompatibility, with no adverse host tissue reactions at 3 and 6 months. Similarly, the group also reported both excellent host response and no indication of inflammatory response at 2 years according to histological results. Thus, gradual and late molecular weight decreases combined with excellent long term biocompatibility and bone regeneration were suggested for PCL based scaffolds. However, in vivo absorption of low molecular weight PCL (3000) was also shown to involve intracellular phagocytosis mainly by phagocytes and giant cells [42]. Hence, PCL implants could be expected to show foreign body reaction when polymer degrades to such low molecular weight. Yet, it was also shown that PCL with this molecular weight was metabolized and excreted from the body and did not accumulate in any organs [33]. In our SEM results the interface of DBM containing implants had a continuous appearance with the bone tissue (Figs. 11e and 12c, g, k) and a direct bone apposition with excellent bone-implant integrity. Active bone formation was more evident around the PCL/BG, PCL/BG/CS and PCL/BG/DBM implant sites and interpreted as a result of osteoinductive and osteoconductive properties of BG, CS and DBM components [43]. The slower resorption of BG caused an ongoing homogeneous bone formation around the implant site. At PCL/BG/CS bone-implant interface showed less osteoconduction (Fig. 12 f, j) than observed with DBM (Fig 12 g, k) probably owing to contiuous elution of CS from the implants. This result was in parallel with the lower microhardness values at the interface I regions of CS containing group (Fig. 10a). It was shown that the degradation of CS had a chemical dissolution character rather than cell-mediated resorption/phagocytosis [44] and dissolved CS serves as a concentrated source of calcium for bone mineralization [45]. Therefore, CS increased the rate of osteogenesis at bone implant interface II (Fig. 10b) but not at interface I due to the unstable PCL/BG/CS surface.

5 Conclusıons

PCL/BG based composites with DBM or CS as third component were prepared by compression moulding without the use of solvent and high temperature. The third

components were shown to improve degradation rate, biocompatibility, bioactivity as well as initial mechanical properties of implants in vitro. Although in vivo results did not reach to statistically significant levels due to limited sample size and high degree of variability observed with living organisms, bone ingrowth and new bone formation at the interface were enhanced with the third components (mainly with DBM) through microhardness, QCT and histological evaluations.

Acknowledgements This study was supported by the Scientific and Technological Research Council of Turkey, TUBITAK (Project no: 104M172).

References

1. Coetzee AS. Regeneration of bone in the presence of calcium sulfate. Arch Otolaryngol. 1980;106:405–9.
2. Stubbs D, Deakin M, Chapman-Sheath P, Bruce W, Debes J, Gillies RM, et al. In vivo evaluation of resorbable bone graft substitutes in a rabbit tibial defect model. Biomaterials. 2004;25(20):5037–44.
3. Abjornson C, Lane JM. Demineralized bone matrix and synthetic bone graft substitutes. In: Friedlaender GE, Mankin HJ, Goldberg VM, editors. Bone grafts and bone graft substitutes. Rosemont: American Academy of Orthopaedic Surgeons; 2006. p. 9–20.
4. Cook SD, Salkeld SL, Patron LP, Barrack RL. The effect of demineralized bone matrix gel on bone ingrowth and fixation of porous implants. J Arthroplasty. 2002;17:402–8.
5. Calandrelli L, Immirzi B, Malinconico M, Volpe MG, Oliva A, Della Ragione F. Preparation and characterisation of composites based on biodegradable polymers for *in vivo* application. Polymer. 2000;41:8027–33.
6. Lu HH, Tang A, Oh SC, Spalazzi JP, Dionisio K. Compositional effects on the formation of a calcium phosphate layer and the response of osteoblast-like cells on polymer-bioactive glass composites. Biomaterials. 2005;26:6323–34.
7. Chouzouri G, Xanthos M. In vitro bioactivity and degradation of polycaprolactone composites containing silicate fillers. Acta Biomater. 2007;3:745–56.
8. Prabhakar RL, Brocchini S, Knowles JC. Effect of glass composition on the degradation properties and ion release characteristics of phosphate glass-polycaprolactone composites. Biomaterials. 2005;26:2209–18.
9. Hao J, Yuan M, Deng X. Biodegradable and biocompatible nanocomposites of poly(ε-caprolactone) with hydroxyapatite nanocrystals: thermal and mechanical properties. J Appl Polym Sci. 2002;86:676–83.
10. Kim BK, Hwang SJ, Park JB, Park HJ. Characteristics of felodipine-located poly(-caprolactone) microspheres. J Microencapsulation. 2005;22:193–203.
11. Rai B, Teoh SH, Ho KH. The effect of rhBMP-2 on canine osteoblasts seeded onto 3D bioactive polycaprolactone scaffolds. Biomaterials. 2004;25:5499–506.
12. Pitt C. Poly(ε-caprolactone) and its copolymers. In: Chasin M, Langer R, editors. Biodegradable polymers as drug delivery systems. New York: Marcel-dekker; 1990. p. 71–120.
13. Coombes AGA, Rizzi SC, Williamson M, Barralet JE, Downes S, Wallace WA. Precipitation casting of polycaprolactone for applications in tissue engineering and drug delivery. Biomaterials. 2004;25:315–25.
14. Mano JF, Sousa RA, Boesel LF, Neves NM, Reis RL. Bioinert, biodegradable and injectable polymeric matrix composites for hard tissue replacement: state of the art and recent developments. Compos Sci Technol. 2004;64:789–817.
15. Azevedo MC, Reis RL, Claase MB, Grijpma DW, Feijen J. Development and properties of polycaprolactone/hydroxyapatite composite biomaterials. J Mater Sci: Mater Med. 2003;14:103–7.
16. Jukola H, Nikkola L, Gomes ME, Chiellini F, Tukiainen M, Kellomäki M, et al. Development of a bioactive glass fiber reinforced starch–polycaprolactone composite. J Biomed Mater Res Part B: Appl Biomater. 2008;87:197–203.
17. Jiang G, Evans ME, Jones IA, Rudd CD, Scotchford CA, Walker GS. Preparation of poly(e-caprolactone)/continuous bioglass fibre composite using monomer transfer moulding for bone implant. Biomaterials. 2005;26:2281–8.
18. Lei Y, Rai B, Ho KH, Teoh SH. In vitro degradation of novel bioactive polycaprolactone—20% tricalcium phosphate composite scaffolds for bone engineering. Mater Sci Eng C. 2007;27:293–8.
19. Yuan H, de Bruijn JD, Zhang X, van Blitterswijk CA, de Groot K. Bone induction by porous glass ceramic made from bioglass (45S5). J Biomed Mater Res (Appl Biomater). 2001;58:270–6.
20. Chan C, Thompson I, Robinson P, Wilson J, Hench L. Evaluation of bioglass/dextran composite as a bone graft substitute. Int J Oral and Maxillofac Surg. 2002;31:73–7.
21. Oliva A, Salerno A, Locardi B, Riccio V, Della Ragione F, Iardino P, et al. Behaviour of human osteoblasts cultured on bioactive glass coatings. Biomaterials. 1998;19:1019–25.
22. Shapoff CA, Alexander DC, Clark AE. Clinical use of a bioactive glass particulate in the treatment of human osseous defects. Compend Contin Educ Dent. 1997;18:356–63.
23. Müller L, Müller FA. Preparation of SBF with different HCO_3^- content and its influence on the composition of biomimetic apatites. Acta Biomater. 2006;2:181–9.
24. Fini M, Giavaresi G, Aldini NN, Torricelli P, Botter R, Beruto D, et al. A bone substitute composed of polymethylmethacrylate and a-tricalcium phosphate: results in terms of osteoblast function and bone tissue formation. Biomaterials. 2002;23:4523–31.
25. Furumatsu T, Shen ZN, Kawai A, Nishida K, Manabe H, Oohashi T, et al. Vascular endothelial growth factor principally acts as the main angiogenic factor in the early stage of human osteoblastogenesis. J Biochem. 2003;133:633–9.
26. Shao XX, Hutmacher DW, Ho ST, Goh JCH, Lee EH. Evaluation of a hybrid scaffold/cell construct in repair of high-load-bearing osteochondral defects in rabbits. Biomaterials. 2006;27:1071–80.
27. Gu YW, Tay BY, Lim CS, Yong MS. Biomimetic deposition of apatite coating on surface-modified NiTi alloy. Biomaterials. 2005;26:6916–23.
28. Feng B, Chen JY, Qi SK, He L, Zhao JZ, Zhang XD. Characterization of surface oxide films on titanium and bioactivity. J Mater Sci: Mater Med. 2002;13:457–64.
29. Kokubo T, Kim HM, Kawashita M. Novel bioactive materials with different mechanical properties. Biomaterials. 2003;24:2161–75.
30. Maeda H, Maquet V, Chen QZ, Kasuga T, Jawad H, Boccaccini AR. Bioactive coatings by vaterite deposition on polymer substrates of different composition and morphology. Mater Sci Eng C. 2007;27:741–5.
31. Xin R, Leng Y, Chen J, Zhang Q. A comparative study of calcium phosphate formation on bioceramics in vitro and in vivo. Biomaterials. 2005;26:6477–86.
32. Han B, Yang Z, Nimni M. Effects of moisture and temperature on the osteoinductivity of demineralized bone matrix. J Orthop Res. 2005;23:855–61.

33. Sun H, Mei L, Song C, Cui X, Wang P. The in vivo degradation, absorption and excretion of PCL-based implant. Biomaterials. 2006;27:1735–40.
34. Yeo A, Rai B, Sju E, Cheong JJ, Teoh SH. The degradation profile of novel, bioresorbable PCL-TCP scaffolds: an in vitro and in vivo study. J Biomed Mater Res. 2008;84A:208–18.
35. Clark PA, Moioli EK, Sumner DR, Mao JJ. Porous implants as drug delivery vehicles to augment host tissue integration. FASEB J. 2008;22:1684–93.
36. Doblaré M, García JM, Gómez MJ. Modelling bone tissue fracture and healing: a review. Eng Fract Mech. 2004;71:1809–40.
37. Aldini NN, Fini M, Giavaresi G, Torricelli P, Martini L, Giardino R, et al. Improvement in zirconia osseointegration by means of a biological glass coating: an in vitro and in vivo investigation. J Biomed Mater Res. 2002;61A:282–9.
38. Lowry KJ, Hamson KR, Bear L, Peng YB, Calaluce R, Evans ML, et al. Polycaprolactone/glass bioabsorbable implant in a rabbit humerus fracture model. J Biomed Mater Res. 1997;36: 536–41.
39. Savarino L, Baldini N, Greco M, Capitani O, Pinna S, Valentini S, et al. The performance of poly-e-caprolactone scaffolds in a rabbit femur model with and without autologous stromal cells and BMP4. Biomaterials. 2007;28:3101–9.
40. Oh SH, Park IK, Kim JM, Lee JH. In vitro and in vivo characteristics of PCL scaffolds with pore size gradient fabricated by a centrifugation method. Biomaterials. 2007;28:1664–71.
41. Lam CXF, Hutmacher DW, Schantz JT, Woodruff MA, Teoh SH. Evaluation of polycaprolactone scaffold degradation for 6 months in vitro and in vivo. J Biomed Mater Res. 2009;90A: 906–19.
42. Woodward SC, Brewer PS, Moatamed F, Schindler A, Pitt CG. The intracellular degradation of poly (epsilon-caprolactone). J Biomed Mater Res. 1985;19:437–44.
43. Moimas L, Biasotto M, di Lenarda R, Olivo A, Schmid C. Rabbit pilot study on the resorbability of three-dimensional bioactive glass fibre scaffolds. Acta Biomater. 2006;2:191–9.
44. Hing KA, Wilson LF, Buckland T. Comparative performance of three ceramic bone graft substitutes. The Spine J. 2007;7:475–90.
45. Al Ruhaimi KA. Effect of calcium sulphate on the rate of osteogenesis in distracted bone. Int J Oral Maxillofac Surg. 2001; 30:228–33.